Article

Detection and Automatic Repair of Nucleotide Base-Pair Mutations by Coherent Light

Ioannis Thanopulos, and Moshe Shapiro

J. Am. Chem. Soc., **2005**, 127 (41), 14434-14438• DOI: 10.1021/ja053396t • Publication Date (Web): 27 September 2005

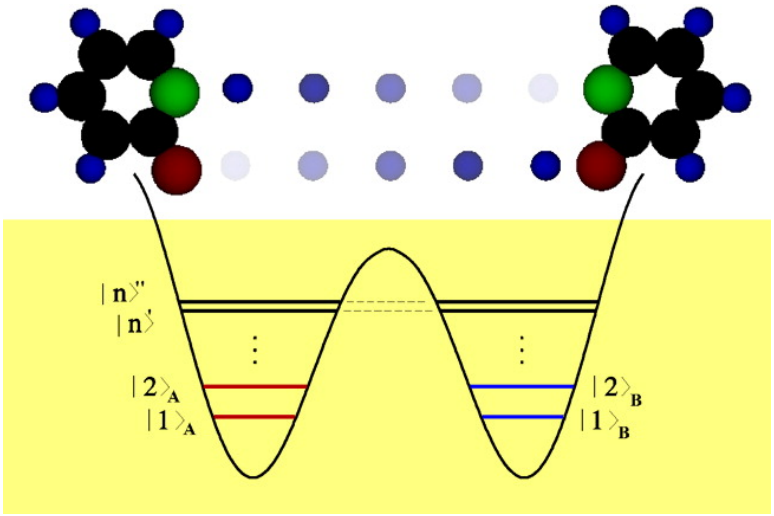

More About This Article

Additional resources and features associated with this article are available within the HTML version:

- Supporting Information
- Access to high resolution figures
- Links to articles and content related to this article
- Copyright permission to reproduce figures and/or text from this article

View the Full Text HTML

J|A|C|S
ARTICLES
Published on Web 09/27/2005

Detection and Automatic Repair of Nucleotide Base-Pair Mutations by Coherent Light

Ioannis Thanopulos*,† and Moshe Shapiro†,‡

Contribution from the Department of Chemistry, The University of British Columbia, Vancouver V6T1Z1, Canada, and Department of Chemical Physics, The Weizmann Institute, Rehovot 76100, Israel

Received May 24, 2005; E-mail: ioannis@chem.ubc.ca

Abstract: We show that phase-coherent optical techniques allow for the detection and automatic repair of mutations in nucleotide pairs. We demonstrate computationally that there is a laser pulse sequence that can detect the occurrence of a mutation caused by a double proton transfer between hydrogen-bonded nucleotide pairs and automatically repair it by converting the mutated nucleotide pair to the nonmutated one. The specific system chosen for this demonstration is the hydrogen-bonded 2-pyridone·2-hydroxypyridine dimer at typical internucleotide distances, a well-established model for tautomeric acid base pairs.

I. Introduction

Hydrogen bonding between nucleotide pairs is a major factor in the observed stability and fidelity of replication of DNA.[1,2] It has been recognized for quite some time that double proton transfer between hydrogen-bonded dinucleotides can transform one dinucleotide pair to another, leading to loss of recognition of the correct base pair in DNA and RNA. For example, proton transfer in the Guanine-Cytosine (G·C) pair is considered a crucial part of the radiation-induced damage to DNA.[3,4]

The mechanism of the tautomerization of hydrogen-bonded base-pairs, induced by double proton transfer (DPT) from one stable configuration A to another (almost energetically equivalent) stable configuration B, in either a sequential or concerted fashion, has been extensively discussed in the literature.[5−17] Control over the DPT process is a major objective, as well as techniques that would enable the detection and repair of an undesired tautomerization once it has occurred.[18]

The object of this paper is to show that control of such a process can be achieved with optical means, using *Coherent Control* (CC)[19] techniques. CC is based on guiding a material system (employing "tailor-made" external laser fields) to arrive at a given final state via a number of indistinguishable quantum pathways. It has been amply documented, both experimentally and theoretically,[20−25] that *selectivity* in a host of physical and chemical processes can be achieved by controlling the interference between such quantum pathways. For example, inducing constructive interference between pathways leading to the same product enhances a desired outcome, whereas destructive quantum interferences lead to the suppression of undesired future events.

A complementary process, in which the material system is guided in an adiabatic fashion along a single pathway (termed "Adiabatic Passage" (AP)[26−28]), enables one to transfer populations in a *complete* way from one state to another. The merging of the two techniques, appropriately named "Coherently Controlled Adiabatic Passage" (CCAP), achieving both *selectivity* and *completeness* has been recently accomplished.[29−31]

† The University of British Columbia.
‡ The Weizmann Institute.

(1) Jeffrey, G.; Saenger, W. *Hydrogen Bonding in Biological Structures;* Springer: Berlin, 1991.
(2) Lehninger, A.; Nelson, D.; Cox, M. *Principles of Biochemistry;* Worth Publishers: New York, 1987.
(3) Nir, E.; Kleinermanns, K.; de Vries, M. *Nature* **2000**, *408*, 949.
(4) Nir, E.; Kleinermanns, K.; Grace, L.; de Vries, M. *J. Phys. Chem. A* **2001**, *105*, 5106.
(5) Rini, M.; Magnes, B.-Z.; Pines, E.; Nibbering, E. *Science* **2003**, *301*, 349.
(6) Folmer, D.; Wisniewski, E.; Hurley, S.; Castlemann, A., Jr. *Proc. Natl. Acad. Sci. U.S.A.* **1999**, *96*, 12980.
(7) Catalán, J.; Pérez, P.; del Valle, J.; de Paz, J.; Kasha, M. *Proc. Natl. Acad. Sci. U.S.A.* **2004**, *101*, 419.
(8) Voegel, J.; Benner, S. *J. Am. Chem. Soc.* **1994**, *116*, 6929.
(9) Guallar, V.; Douhal, A.; Moreno, M.; Lluch, J. *J. Phys. Chem. A* **1999**, *103*, 6251.
(10) Borst, D.; Roscioli, J.; Pratt, D.; Florio, G.; Zwier, T.; Müller, A.; Leutwyler, S. *Chem. Phys. Lett.* **2002**, *283*, 341.
(11) Müller, A.; Talbot, F.; Leutwyler, S. *J. Chem. Phys.* **2001**, *115*, 5192.
(12) Meuwly, M.; Müller, A.; Leutwyler, S. *Phys. Chem. Chem. Phys.* **2003**, *5*, 2663.
(13) Frey, J.; Müller, A.; Frey, H.-M.; Leutwyler, S. *J. Chem. Phys.* **2004**, *121*, 8237.
(14) Tautermann, C.; Voegele, A.; Liedl, K. *Chem. Phys. Lett.* **2003**, *292*, 47.
(15) Smedarchina, Z.; Siebrand, W.; Fernadez-Ramos, A.; Martinez-Nunez, E. *Chem. Phys. Lett.* **2004**, *386*, 396.
(16) Roscioli, J.; Pratt, D.; Smedarchina, Z.; Siebrand, W.; Fernandez-Ramos, A. *J. Chem. Phys.* **2004**, *120*, 11351.
(17) Zoete, V.; Meuwly, M. *J. Chem. Phys.* **2004**, *121*, 4377.
(18) Schultz, T.; Samoylova, E.; Radloff, W.; Hertel, I.; Sobolewski, A.; Domcke, W. *Science* **2004**, *306*, 1765.
(19) Shapiro, M.; Brumer, P. *Principles of the Quantum Control of Molecular Processes;* John Wiley & Sons: New Jersey, 2003.
(20) Zare, R. *Science* **1998**, *279*, 1875.
(21) Weinacht, T.; Ahn, J.; Bucksbaum, P. *Nature* **1999**, *397*, 233.
(22) Meshulach, D.; Silberberg, Y. *Nature* **1998**, *396*, 239.
(23) Brixner, T.; Bamrauer, N.; Nicklaus, P.; Gerber, G. *Nature* **2001**, *414*, 57.
(24) Rabitz, H.; Hsieh, M.; Rosenthal, C. *Science* **2004**, *303*, 1998.
(25) Herek, J.; Wohlleben, W.; Cogdell, R.; Zeidler, D.; Motzkus, M. *Nature* **2002**, *417*, 533.
(26) Oreg, J.; Hioe, F.; Eberly, J. *Phys. Rev. A* **1984**, *29*, 690.
(27) Gaubatz, U.; Rudecki, P.; Schiemann, S.; Bergmann, K. *J. Chem. Phys.* **1990**, *92*, 5363.
(28) Vitanov, N.; Fleischhauer, M.; Shore, B.; Bergmann, K. *Adv. At. Mol. Opt. Phys.* **2001**, *46*, 55.
(29) Kral, P.; Shapiro, M. *Phys. Rev. Lett.* **2001**, *87*, 183002.
(30) Kral, P.; Thanopulos, I.; Shapiro, M.; Cohen, D. *Phys. Rev. Lett.* **2003**, *90*, 033001.
(31) Thanopulos, I.; Kral, P.; Shapiro, M. *J. Phys. Chem.* **2003**, *119*, 5105.

10.1021/ja053396t CCC: $30.25

Figure 1. Dinucleotide dimer. The double proton (cyan) transfer takes place between the two nitrogen atoms (green) and the two oxygen atoms (red).

In this paper we demonstrate by computational means that the CCAP method enables one to both distinguish between base-pairs residing in two energetically equivalent A and B minima, as well as induce and control the interconversion of the system between these two configurations. This demonstration gives rise to the hope that we would in the future be able to detect, as well as correct by purely optical means, undesired mutagenesis and manipulate genomes in a sequence-specific manner.

II. Dinucleotide Pair Model System

As a vehicle for this demonstration we choose the well studied[10−12,14−16] nucleic acid base-pair model the 2-pyridone (2PY) and 2-hydroxypiridine (2HP) dimer (shown in Figure 1) embedded in a "pocket" of a nucleic acid. We keep the dimer at a separation similar to that found in nucleic acids, where the base-pair members are unable to approach each other too closely due to their attachments to the nucleotide backbone.[17] In this way we slow the natural rate of DPT tunneling in isolated dimers, in keeping with environments typical of base pairs embedded in nucleic acids.

The concerted motion of the two protons during the 2PY·2HP tautomerization process may be described as a motion along a *linear reaction path*[32] connecting the two equilibrium configurations A and B. This path is given as

$$\vec{R}_i(s) = \frac{1}{2}(\vec{R}_i^{A} + \vec{R}_i^{B}) + s(\vec{R}_i^{B} - \vec{R}_i^{A}) \qquad (1)$$

where $\vec{R}_i^k$ denotes the three-dimensional Cartesian coordinate vector of the i-th atom in the molecular center-of-mass frame for the (k = A, B) equilibrium structures. The parameter $-0.825 \le s \le 0.825$ describes the position of the system along the reaction path, with the A tautomer corresponding to $s = -0.5$, the B tautomer corresponding to $s = 0.5$, and the "transition state" corresponding to $s = 0$. This type of path is particularly suitable for studying the transfer of light particles between two heavier moieties,[32] which are thus naturally kept immobile.

The potential energy and the molecular structures are obtained in an ab initio way using the hybrid B3LYP density functional (DFT) method and the valence triple-ζ 6-311++G(d,p) basis set of the *Gaussian98* electronic structure calculation package.[33] The two equilibrium configurations of the dimer are planar in the (x,y) plane at this level of ab initio theory, and consequently the linear reaction path from A to B is planar as well.

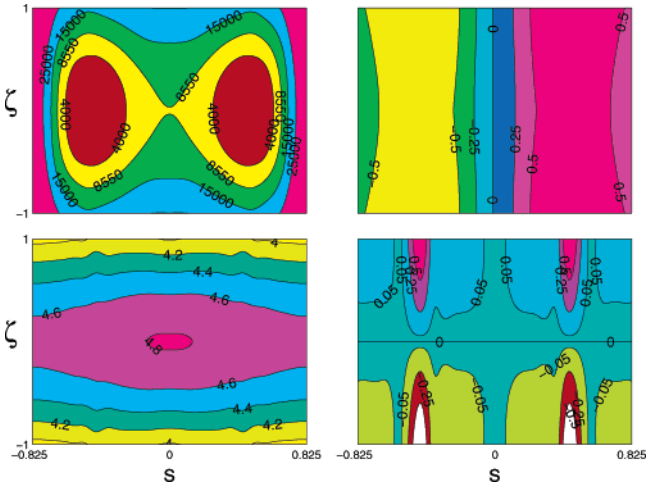

Figure 2. Potential and electric dipole surfaces of our model. Upper panels: The two-dimensional potential energy surface (left) and the surface for the x component of the electric dipole (right). Lower panels: The two-dimensional surfaces for the y (left) and z (right) components of the electric dipole.

In addition to the in-plane motion we also consider the out-of-plane vibration that involves out-of-phase motions of the hydrogen atoms as the system propagates along the reaction path.[34] This out-of-plane motion is parametrized by a variable $-1 \le \zeta \le 1$. Our working space is thus confined to the $\{(s,\zeta) \in [-0.825, 0.825] \times [-1, 1]\}$ two-dimensional part of the dimer configuration space. This is the minimal space needed to properly describe the dynamics of our control scheme using the energetically lowest states of the dimer.

Our calculations yield a linear reaction path potential energy barrier height of ∼8550 cm^{-1}. Our two-dimensional configuration space model predicts tunneling times from A to B of ∼0.3 μs. Although this is still much shorter than the estimated tunneling times in nucleic acids,[35] which may be also due to the fact that B3LYP in general underestimates energy barriers for proton transfer, it is by far longer than the tunneling times in the isolated unconstrained dimers where the monomers are allowed to get much closer to one another.[15,16] As shown in the following, this tunneling time is sufficiently long to allow us to consider the localized states at the A or B minima as "legitimate" initial or final states. Our calculated potential energy and electric dipole surfaces in the $\{s,\zeta\}$ space are shown in Figure 2. The fact that there exist degenerate A and B tautomers makes the separate addressing of these tautomers by optical means difficult. We have overcome this difficulty using a two-step approach: In the first step we affect the *discrimination* between the tautomers. In the second step we use the discrimination afforded by the first step to control the *interconversion* between the tautomers. The discrimination step[29−31] makes use of the different symmetries of the x, y, and z components of the dipole moment to manipulate molecules in configuration A and B differently. As can be seen in Figure 2, the x component of the electric dipole is symmetric with respect to ζ inversion and antisymmetric with respect to s inversion; the z component

(32) Miller, W.; Ruf, B.; Chang, Y.-T. *J. Phys. Chem.* **1988**, *89*, 6298.
(33) Frisch, M. J.; Trucks, G. W.; Schlegel, H. B.; Scuseria, G. E.; Robb, M. A.; Cheeseman, J. R.; Zakrzewski, V. G.; Montgomery, J. A., Jr.; Stratmann, R. E.; Burant, J. C.; Dapprich, S.; Millam, J. M.; Daniels, A. D.; Kudin, K. N.; Strain, M. C.; Farkas, O.; Tomasi, J.; Barone, V.; Cossi, M.; Cammi, R.; Mennucci, B.; Pomelli, C.; Adamo, C.; Clifford, S.; Ochterski, J.; Petersson, G. A.; Ayala, P. Y.; Cui, Q.; Morokuma, K.; Malick, D. K.; Rabuck, A. D.; Raghavachari, K.; Foresman, J. B.; Cioslowski, J.; Ortiz, J. V.; Stefanov, B. B.; Liu, G.; Liashenko, A.; Piskorz, P.; Komaromi, I.; Gomperts, R.; Martin, R. L.; Fox, D. J.; Keith, T.; Al-Laham, M. A.; Peng, C. Y.; Nanayakkara, A.; Gonzalez, C.; Challacombe, M.; Gill, P. M. W.; Johnson, B. G.; Chen, W.; Wong, M. W.; Andres, J. L.; Head-Gordon, M.; Replogle, E. S.; Pople, J. A. *Gaussian 98*, revision A.11; Gaussian, Inc.: Pittsburgh, PA, 2001.
(34) The instantaneous out-of-plane normal mode along the linear reaction path is chosen in such a way that overlaps maximally with the $\nu_{28} \approx 932$ cm^{-1} normal mode of the equilibrium configuration A or B.
(35) Löwdin, P.-O. *Rev. Mod. Phys.* **1963**, *35*, 724.

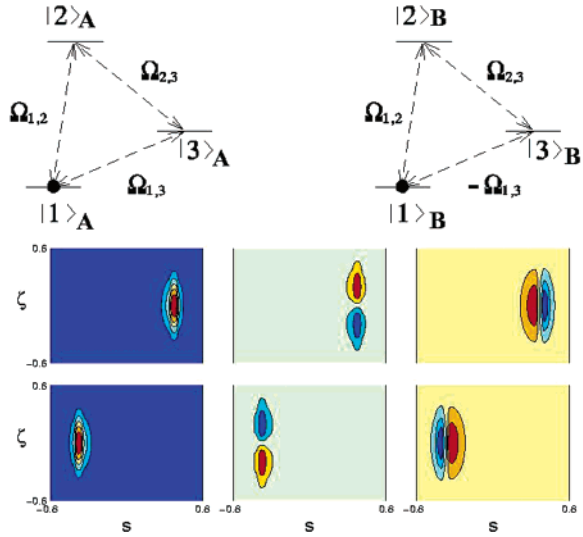

Figure 3. Detection scheme. Top panel: The coupling scheme for the discriminator. Middle panels: The $|j\rangle_B$, ($j = 1, 2, 3$) localized states (left to right). Bottom panels: The $|j\rangle_A$, ($j = 1, 2, 3$) localized states (left to right).

behaves in the opposite manner; and the y component is symmetric with respect to inversion of ζ or s.

III. Detection and Automatic Repair

The cyclic laser coupling scheme, which is at the heart of the first "discrimination" step, is depicted in the upper part of Figure 3. As shown in the figure, the laser fields inter-couple three vibrational states of the A tautomer, as well as inter-couple separately three vibrational states of the B tautomer. As discussed below, we can, by controlling one overall phase of the laser fields,[29−31] excite only the $|1\rangle_B$ ground state to a higher $|i\rangle_B$ vibrational state of the B tautomer, while leaving all the A-tautomer states untouched.

Following this selective excitation, it is now possible to transfer in the second step the $|1\rangle_A$ (ground state of the A tautomer) population, if such exists, to a $|j\rangle_B \neq |i\rangle_B$ B-tautomer excited state. In this way, any population residing initially in $|1\rangle_A$ is automatically converted to the B tautomer. Thus, we are able both to detect the existence of a mutation *and* to repair it automatically.

Moreover, if it is the A tautomer that we desire, we can, by tuning the overall laser phase, interchange the process, with the excitation of the B states switched over to the excitation of the A states and the transfer occurring from B to A.

IV. Dynamics of Detection

We now present a numerical demonstration of the detection scheme. As our localized vibrational states we use the three lowest, $\{|1\rangle_k, |2\rangle_k, |3\rangle_k\}$, $k =$ A, B tautomeric states. The two-dimensional $\{s,\zeta\}$ configuration space wave functions, corresponding to these six localized states, are shown in the middle and bottom panels of Figure 3. Each of the above localized states is a superposition of an $|i'\rangle$ and an $|i''\rangle$ vibrational eigenstate,

$$|i\rangle_k = \frac{1}{\sqrt{2}}(|i'\rangle \pm |i''\rangle), \qquad k = \text{A, B} \tag{2}$$

where $|i'\rangle$ denotes the s-symmetric i-th vibrational eigenstate, and $|i''\rangle$, the s-antisymmetric i-th eigenstate. Since the dimer in our study is assumed to represent a base pair confined to a "pocket" of a nucleic acid, we are justified in neglecting the rotational motion of the dimer.

According to our calculations,[36] the tunneling splittings between the $|i'\rangle$ and $|i''\rangle$ eigenstates for the first three doublets ($i = 1, 2, 3$) are 10^{-4} cm^{-1}, 3×10^{-4} cm^{-1} and 10^{-3} cm^{-1}, respectively. These numbers imply that the interconversion times between the $|i\rangle_A$ and $|i\rangle_B$ ($i = 1, 2, 3$) localized states are roughly 150, 50, and 15 ns, respectively. The laser pulses for our two-step control scheme, "discriminator" and "converter" in tandem, are of total duration ~300 ps, which is much shorter than the tunneling interconversion times, thus justifying the assumption that the localized states are well-defined physical entities.

The "discrimination" step depends on the Rabi frequencies associated with each pulse, $\Omega_{ij} = \vec{\mu}_{i,j}\cdot\vec{E}(t) = \Omega_{ij}^{\max} f_{i,j}^{l}(t)$, where $\vec{\mu}_{i,j}$ is the electric dipole moment for the $i \leftarrow j$ transition and $\vec{E}(t)$ is the electric field of the laser pulse. The time dependence of Ω_{ij} is given by the pulse shape function $f_{ij}^{l}(t)$, shown in the upper panel of Figure 4 for the polarizations used.

The primary factor that allows us to distinguish between the case where the population resides initially in tautomer A and the case where it resides initially in tautomer B is the phase of the product of the three (complex) Rabi frequencies $\Omega_{23}^{k}\Omega_{13}^{k}\Omega_{12}^{k}$($k =$ A, B). As shown elsewhere,[29−31] by merely changing this phase by π we determine whether it is the A or the B tautomeric states that are to be affected by the lasers. Here, a π-phase dependence originates in the different symmetry properties of the electric dipole component of the dimer, shown in Figure 2. Due to these different directional properties of the dipole moments, choosing the polarization of the pulse coupling of the $|1\rangle_k$ and $|3\rangle_k$ ($k =$ A, B) states to lie along the x-direction and that of the two other pulses to lie along the z-direction, results in $\Omega_{1,2}^{A} = \Omega_{1,2}^{B}$, $\Omega_{2,3}^{A} = \Omega_{2,3}^{B}$, and $\Omega_{1,3}^{A} = -\Omega_{1,3}^{B}$. Hence there exists a π phase difference in the product of the Rabi frequencies as seen by the A tautomer relative to that seen by the B tautomer. The discrimination process described above is therefore possible.

Our numerical simulations, with electric dipole matrix elements for the relevant $i \leftarrow j$ transitions being ~0.01 D and the chosen pulse intensities yielding $\Omega_{ij}^{\max} \approx 1$ ps^{-1}, are plotted in Figure 4. As demonstrated in the upper panel, to attain complete population transfer by adiabatic passage, we apply the pulses in a "counterintuitive" order.[27,28] By the term "counterintuitive"

(36) The vibrational eigenstates in the $\{s,\zeta\}$ configuration space are obtained in the Discrete Variable Representation (DVR) (for a review see ref 39) by solving the corresponding Schrödinger equation with a Hamiltonian for the generalized coordinates[40] $q_1 = s$ and $q_2 = \zeta$.

$$H = \frac{1}{2}\sum_{q_1,q_2} \partial_{q_1}^{*} G_{q_1q_2}(s,\zeta)\partial_{q_2} + u(s,\zeta) + V(s,\zeta) \tag{4}$$

Here, V is the potential energy of the ground electronic state of Figure 2 and u is the "pseudopotential"

$$u(s,\zeta) = \frac{\hbar^2}{8}\sum_{q_1,q_2}\frac{\partial}{\partial q_1}\left\{G_{q_1q_2}\frac{\partial \ln|\mathbf{g}|}{\partial q_2}\right\} + \frac{1}{4}\frac{\partial \ln|\mathbf{g}|}{\partial q_1}G_{q_1q_2}\frac{\partial \ln|\mathbf{g}|}{\partial q_2}$$

where $\mathbf{g}$ is the covariant and $\mathbf{G}$ is the contravariant metric tensor, respectively, given by

$$g_{q_1q_2} = m_a\frac{\partial \vec{x}_a}{\partial q_1}\cdot\frac{\partial \vec{x}_a}{\partial q_2}, G_{q_1q_2} = m_a^{-1}\frac{\partial q_1}{\partial \vec{x}_a}\cdot\frac{\partial q_2}{\partial \vec{x}_a} \tag{5}$$

and $|\mathbf{g}|$ is the determinant of $\mathbf{g}$. In the above equations, where summation over dummy indices is implicitly understood, m_a is the mass of the a-th atom in the dimer, $\vec{e}_\alpha$ ($\alpha = x, y, z$) are the unit vectors in the center-of-mass molecule-fixed frame, and $\vec{x}_a$ denotes the Cartesian coordinate vector of the a-th atom in this frame.

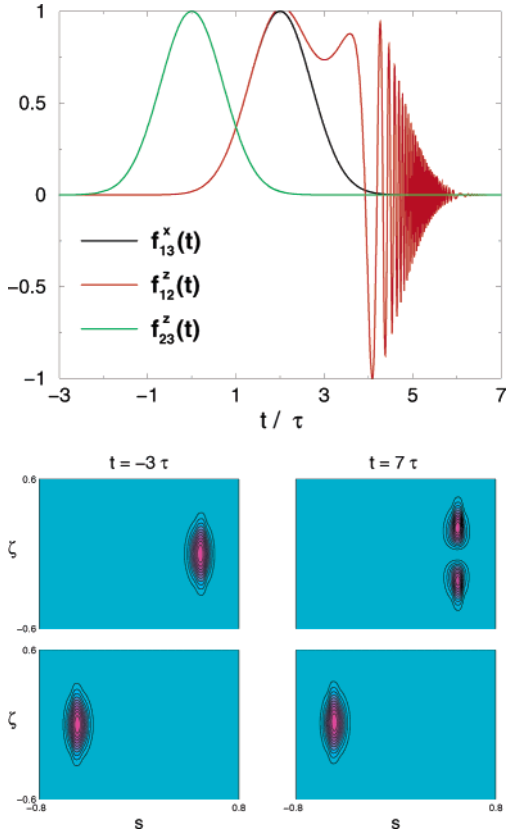

Figure 4. Detection scheme dynamics. Upper panel: The pulse shape functions $f^{l}_{ij}(t)$ for the laser fields coupling resonantly the localized $|i\rangle_k$ and the $|j\rangle_k$ k = A, B states. The polarization is denoted as l ($l = x, z$). Middle panels: The initial ($t = -3\tau$) and final ($t = 7\tau$) wave functions in configuration B. Bottom panels: the same for the A configuration.

we mean that the $\Omega^z_{2,3}(t)$ "dump" pulse is applied before the $\Omega^x_{1,3}(t)$ and $\Omega^z_{1,2}(t)$ "pump" pulses. In addition, the $\Omega^z_{1,2}(t)$ pulse has to last longer than the $\Omega^x_{1,3}(t)$ pulse, and its late part be chirped[29−31] according to $\exp\{-it\Omega^{max}_{12}\exp[-(t-6\tau)^2/\tau^2]\}$.

As shown in the lower panels of Figure 4 by employing the above pulse ordering we can indeed discriminate between the tautomers: At the end of the process the A tautomer is seen to remain in the initially populated (ground) state, while the B tautomer is transferred from its ground state to the $|2\rangle_B$ state. Emptying the ground $|1\rangle_B$ state population, as we have done in the discrimination step, enables us now, in a second step, to exclusively transfer the population from the $|1\rangle_A$ state to the $|3\rangle_B$ state.

V. Automatic Repair Dynamics

The goal of the repair scheme is that the initial population of the $|1\rangle_A$ ground level is transferred to the $|3\rangle_B$ level. The population at the end of the two steps is thus divided between the $|2\rangle_B$ and $|3\rangle_B$ states, thus converting *all* the population from the undesired tautomer A to the desired tautomer B.

This is achieved via a transient excitation to two higher lying eigenstates (shown in Figure 5) that are spaced ∼1.1 cm^{-1} apart, denoted, $|4'\rangle$, which is symmetric, and $|4''\rangle$, which is antisymmetric, with respect to the s reaction coordinate. The electric dipole matrix elements connecting the localized states to these eigenstates have been calculated by us to be ∼0.005 D.

The time dependence of the pulses, hence the Rabi frequencies, is given for the "converter" step as, $\Omega_{1_k4'} = \Omega^{max}_{1_k4'}\exp[-(t-11\tau)^2/\tau^2]$, $\Omega_{3_k4'} = \Omega^{max}_{3_k4'}\exp[-(t-9\tau)^2/\tau^2]$, $|\Omega_{1_k4'}| = |\Omega_{1_k4''}|$ and $|\Omega_{3_k4'}| = |\Omega_{3_k4''}|$, ($k$ = A, B). All the pulses are polarized along the x direction, and $\Omega^{max}_{i4'} \approx 100$ ps^{-1}($i = 1$, 3).

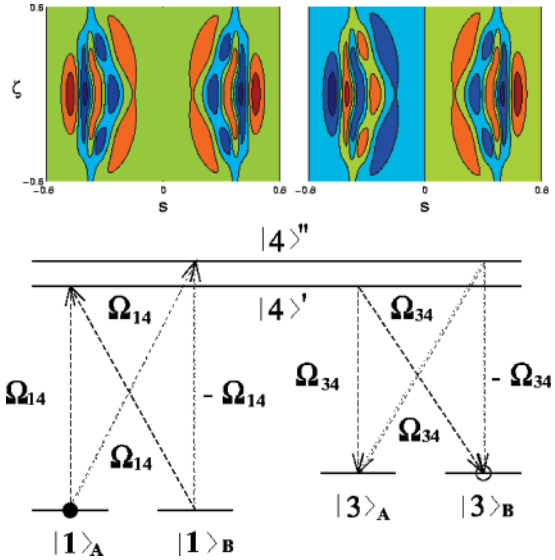

Figure 5. Repair scheme. Upper panels: The eigenfunction of level $|4'\rangle$ (left) and level $|4''\rangle$ (right). Bottom panel: The levels considered and their couplings.

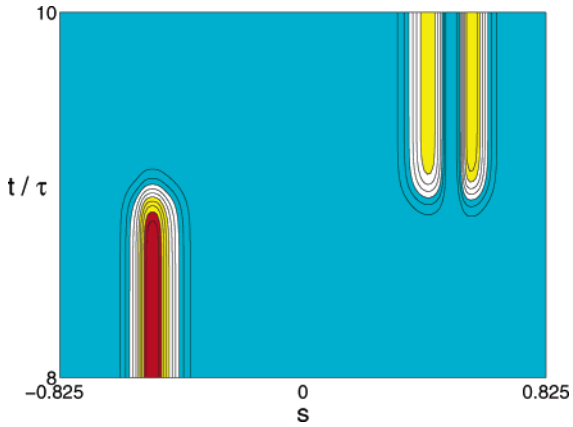

Figure 6. Time evolution of the wave function $\psi(s, t) = \int|\psi(s,\zeta, t)|^2\,d\zeta$ during the "converter" scheme.

In Figure 6 we show the time evolution of the total wave function $|\psi(s,\zeta, t)\rangle = c_{4'}(t)|4'\rangle + c_{4''}(t)|4''\rangle + \sum_{k=A,B}(c_{1_k}(t)|1\rangle_k + c_{3_k}(t)|3\rangle_k)$ during the "converter" step, integrated over the ζ coordinate

$$\psi(s, t) = \int|\psi(s,\zeta, t)|^2\,d\zeta \qquad (3)$$

The population transfer from state $|1\rangle_A$ to state $|3\rangle_B$ is achieved by choosing the pulses in such a way that either $\Omega_{1_k4'}/\Omega_{1_k4''} = -1$ or $\Omega_{3_k4'}/\Omega_{3_k4''} = -1(k$ = A, B).[30,31] We note that, as in other adiabatic passage schemes,[27,28] the $|4'\rangle$ and $|4''\rangle$ states, though being an indispensable part of the "converter" scheme, are never populated during the entire process.[30,31]

VI. Conclusion

We find that, after the "discriminator" and "converter" steps, all the population in tautomer A has been converted to tautomer B. As mentioned above, by simply changing the phase of one of the Rabi frequencies involved, we could equally well have

ended up with only the A tautomer being populated. In fact, our method is capable of purifying a mixture in which there is an initial population in both tautomers. In a complementary way, our approach can be also used on the *single molecule* level to identify, for a given dimer, if the ground-state configuration is that of A or B.

In conclusion, in this paper we have introduced a phase-coherent two-step optical method that enables the direct identification and automatic repair of mutations arising from the misplacement of two protons involved in the hydrogen bonding between two nucleotides. We have demonstrated the process computationally using the 2-pyridone·2-hydroxypyridine dimer. We anticipate that this novel and powerful method will find direct applications in the detection and repair of undesired nucleotide base-pair mutations and in sequence-specific genome targeting for gene modification.[37,38]

JA053396T

(37) Oh, D.; King, B.; Boxer, S.; Hanawalt, P. *Proc. Natl. Acad. Sci. U.S.A.* **2001**, *98*, 11271.
(38) Knauert, M.; Glazer, P. *Hum. Mol. Genet.* **2001**, *10*, 2243.
(39) Light, J.; Carrington, T., Jr. *Adv. Chem. Phys.* **2000**, *114*, 263.
(40) Bunker, P.; Jensen, P. *Molecular Symmetry and Spectroscopy*, 2nd ed.; NRC Research Press: Ottawa, 1998.